Original Article

Textile Research Journal

Textile Research Journal
0(00) 1–12

DOI: 10.1177/0040517513481873
trj.sagepub.com

SAGE

Rheological properties of sodium alginate and xanthan pastes on cotton with reactive dye in screen printing

Lili Wang, Furong Zhu and Danian Lu

Abstract

In this study, sodium alginate (SA) and xanthan (XG), selected as two typical pastes, were intensively investigated by steady, transient, and dynamic rheological methods. Compared with SA, in the steady-shear tests it was found that XG showed a prominent shear-thinning feature at low shear rates and low concentrations. In addition, the transient tests suggested that XG had more remarkable hysteresis thixotropy and that the structural viscosity needed more time to return to its original level after shears. What is more, two pastes in the same concentration performed totally different viscoelastic behaviors from the dynamic tests. SA exhibited more viscous behavior and XG more elastic behavior. Furthermore, experimental data have been correlated with different models: flow curves with the Cross and power-law model, mechanical spectra with the Friedrich–Braun model and Generalized Maxwell model. The relationship between dynamic and steady-shear properties (Cox–Merz rule) was satisfactory for SA while undesirable for XG. Through the rheological properties, it may be inferred that those who show weaker elasticity, stronger viscosity, relatively steady viscoelasticity, and the structural viscosity liable to restore the original level after shears may be more appropriate as the pastes to achieve better printing qualities on cotton printing with reactive dye.

Keywords

Sodium alginate, xanthan, rheological properties, thixotropy, viscoelasticity, screen printing

As an integral part of the printing paste, the thickening agents impart adequate rheological properties in the different flow conditions encountered in the printing process, determining the color yield, levelness, penetration, sharp and clean drawing patterns, and hand. During the printing process, the pastes are forced through the screen openings under high shear rates, deposited onto the fabric, and then will continue to flow at very low shear rates. Yet all the procedures are affected by elastic behavior, dominating the flow behavior and the elastic recovery of the paste instantly after its application. The paste must be characterized by a good screenability and a uniform penetrability into the fabric; moreover, the best sharpness definition must be achieved and the flushing out must be prevented.[1] In many previous studies, major investigations into the rheological behavior of paste had commonly employed steady methods to explore the relations between viscosity and shear stress, and viscosity and temperature.[2–4] However, the transient and dynamic tests were less extensively employed to demonstrate the thixotropic and viscoelastic properties of paste.

The study of the paste rheology is very important. For one thing, paste rheology can give a quantitative description of the paste, which is essential for developing models of various print processing operations. In addition, the models can be employed for quality optimization and for predicting the onset of flow behavior in the printing process. For another, paste rheology can be linked with printer parameters as a quality control tool and for attempting to reduce the associated printing defects in the printing process. Several studies had

Key Laboratory of Science & Technology of Eco-Textile, Ministry of Education, PR China

Corresponding author:
Danian Lu, College of Chemistry, Chemical Engineering & Biotechnology, Donghua University, No. 2999 Ren Min Road (North), Songjiang District, Shanghai, China.
Email: danianlu@163.com

been carried out to elucidate the relations between rheology and printability of conventional printing inks and pastes.[5–7] However, the rheological researches of the pastes still need to be further investigated to clarify the controlling factor dominating the practical screen printing process.

In the natural thickener family, sodium alginate (SA) and xanthan (XG) are excellent thickeners for the application, since they can impart high viscosities at low concentrations and possess adequate rheological behavior.[8,9] At present, SA, a derivative of seaweed, is widely used as thickener in reactive dye printing owing to the good screenability, high color yield, bright color, and soft handle. XG, produced by bacteria of the bacterium *Xanthomonas campestris*, cannot achieve favorable printing qualities, particularly suffering with poor screenability and low color yield. SA is a straight-chain heteropolysaccharide made up of blocks of mannuronic acid and guluronic acid, while XG a branched-chain heteropolysaccharide with a primary structure consisting of repeated pentasaccharide units formed by two glucose units, two mannose units, and one glucuronic acid unit.[10,11] Consequently, there is a large difference of rheological properties between SA and XG. Although the rheological properties of SA and XG have been investigated by several researchers,[12,13] few studies have been implemented regarding the correlation between the rheology and printability of SA and XG. With the developments of new printing technology and fine printing, new demands have been made for the paste rheology.

In this study, the printing qualities using nine polysaccharides as thickeners were first investigated. The quality of textile printing is closely related to the rheological properties of the printing paste, such as fluidity, thixotropy, and viscoelasticity. As a result, SA and XG were selected as two typical pastes that have the best and worst printing qualities, respectively. Their rheological properties have been compared and analyzed by steady, transient, and dynamic methods in order to find the effects of shear actions on the viscous and elastic behaviors for different pastes. What is more, the rheological properties relevant to printing qualities have been tentatively discussed through rheological parameters, such as apparent viscosity (η), storage modulus (G'), loss modulus (G''), loss angle (δ), and complex viscosity (η^*). Different models have also been used to describe the rheological properties for the two pastes.

Experimental details

Materials

All the thickeners were commercial industrial grade. SA was obtained from Jie Crystal Chemical (China) with intrinsic viscosity $11.9\,\mathrm{dL\,g^{-1}}$. KELZAN S XG was provided by CPKELCO (USA) with intrinsic viscosity $19.8\,\mathrm{dL\,g^{-1}}$. The viscosity average molecular weights of SA and XG were 5.95×10^5 and 2.03×10^6, respectively. The average molecular weights were calculated according to the literature.[14,15]

Carboxymethyl starch (CMS) and carboxymethylcellulose (CMC) were produced by Xinfeng Cellulose Factory (China). Flaxseed gum (FG), carrageenan gum (CG), and locust bean gum (LBG) were supplied by Three Good Food Additive (China). Guar gum (GG) and hydroxypropyl guar gum (HGG) were supplied by Guangrao Liuhe Chemicals (China).

The dye used was the monochlorotriazine dye C.I. Reactive Red 245. Other printing paste additives, namely urea and sodium bicarbonate, were supplied by Shanghai Enterprise Group Chemical Reagent (China); reservehao S (sodium-*m*-nitrobenzene sulfonate) was supplied by Shangyu Kangte Chemical (China). Urea is used to increase the solubility of the reactive dye, to accelerate migration of the dye from the thickener film into the fiber, and most importantly for optimal fixation of the reactive dye in superheated steam. Sodium bicarbonate is added to produce ionization of accessible cellulose hydroxyl groups of the fiber, which can react with the reactive dye. Reservehao S is used as the weak oxidizing agent to offset the reactive dye's sensitivity to reduction during steaming.

The printing experiments were performed by using 100% cotton woven fabrics (supplied by Hualun Printing and Dyeing factory, China), which were already pretreated and mercerized. Fabric specifications: thread density $\mathrm{tex} = 14.575\,\mathrm{mg/m}$, warp 13 threads/cm, weft 7 threads/cm.

Preparation of the printing paste and the printing process

The thickener and demineralized water were well stirred in a mixer and put in a refrigerator overnight to attain full swelling. To prepare the printing pastes, $10\,\mathrm{g\,kg^{-1}}$ dyestuff, $10\,\mathrm{g\,kg^{-1}}$ sodium bicarbonate, $50\,\mathrm{g\,kg^{-1}}$ urea, and $10\,\mathrm{g\,kg^{-1}}$ reservehao S were added to the thickener solution and stirred until smooth. All printing pastes were adjusted to viscosity of (10 ± 1) Pa·s at the shear rate $6.25\,\mathrm{s^{-1}}$ at 25°C.

Two patterns, including a $10 \times 10\,\mathrm{cm^2}$ square design and lines of 800 and 200 μm width were printed on cotton fabrics with a laboratory printing machine (Mini MDF R286, Austria KLAGE NFURT), using flat screen 180-mesh and a magnetic-rod diameter of 8 mm at printing speed 6 m/min at the pressure grade 3. The printed square samples were dried for 2 min at 80°C and steamed in a high temperature steam oven (DHE, Switzerland Mathis) for 10 min at 102°C, and

then washed with cold and warm water, respectively, then soaped in boiling water with a bath ratio of 1:50 for 10 min to remove the thickener and unfixed dyes. However, the line samples were only dried for 2 min at 80°C.

Quality-determining parameters

The printing paste add-on was determined gravimetrically from the differences in the mass of cotton fabric samples determined before printing and immediately after the application of the paste.

The color yield, namely K/S, was measured using a color measurement spectrophometer (Datacolor 650, USA).

The color unevenness was calculated for 13 K/S values of the face as follows:

$$\text{Color unevenness (\%)} = \frac{\sqrt{\frac{1}{12}\sum_{i=1}^{13}\left(K/Si - \bar{K}/\bar{S}\right)^2}}{\bar{K}/\bar{S}} \times 100 \quad (1)$$

The width of the line was measured by electron microscopy. The average width and line unevenness were obtained for 30 widths of the printing lines, as follows:

$$\text{Line unevenness (\%)} = \frac{\sqrt{\frac{1}{29}\sum_{i=1}^{30}\left(D_i - \overline{D}\right)^2}}{\overline{D}} \times 100 \quad (2)$$

Rheological measurements

Rheological properties of all samples were measured using a rotational rheometer (ARES-RFS, USA) with cone-and-plate geometry (50 mm diameter, 0.04 radians cone angle, 0.0489 mm gap) at 25 ± 0.01°C. A thin layer of silicone oil was applied on the surface of the samples in order to prevent evaporation.

Steady-shear tests

After the sample was loaded into the rheometer and equilibrated at the testing temperature for 120 s, steady-shear tests were performed over a wide shear rate range of 0.1–1000 s^{-1} to obtain apparent viscosity data versus shear rate.

Transient tests

Thixotropic loop tests. The sample was loaded into the rheometer and equilibrated at the testing temperature for 120 s before measurement. The shear rate was programmed to increase from 0 to 400 s^{-1} in 200 s, then was followed immediately by a decrease from 400 to 0 s^{-1} in the next 200 s.

In-shear structural recovery tests. In-shear structural recovery of the samples was determined according to the procedure of Mezger[16] with some modifications. The sample was placed in the rheometer and equilibrated at the testing temperature for 120 s before measurement. A three-stepped steady-shear test was performed as follows: (1) a constant shear rate of 1 s^{-1} for 120 s and subsequently (2) a constant shear rate of 400 s^{-1} for 60 s and then (3) a constant shear rate of 1 s^{-1} for 120 s. The in-shear recovery value of the sample was calculated as the ratio of average apparent viscosity determined in the third step to the average apparent viscosity obtained in the first step.

Dynamic oscillatory tests. In the oscillatory experiment, paste is exposed to a slight shear deformation within the linear viscoelastic range. The applied strain, γ, and the resultant stress, σ, oscillate sinusoidally with the same angular frequency, ω, expressed as[17]

$$\gamma(t) = \gamma_0 \sin(\omega t) \quad (3)$$

$$\sigma(t) = \sigma_0 \sin(\omega t + \delta) \quad (4)$$

$$G^* = G' + iG'' \quad (5)$$

The ratio of complex stress to complex strain, G^*, is called the complex shear modulus. The storage modulus, G', the real part of the complex shear modulus, is a measurement of the deformation energy, which can be stored reversibly by paste solution, describing the elastic component. On the other hand, loss modulus, G'', the imaginary part of the complex shear modulus, represents a measurement of the energy irreversibly dissipated by viscous flow, standing for the viscous component. The larger G' and G'' are, the more the paste's elasticity, and the worse the flow of paste. Loss angle tangent, tan δ, is used to estimate relative size of elasticity and viscosity. The lower the value of δ is, the more elastic effect the paste performs:

$$\tan\delta = \frac{G''}{G'} \quad (6)$$

Furthermore, a viscosity can also be obtained by oscillation experiment, calculated from the complex shear modulus, describing a viscosity as would be expected from the solution structure of the relaxed state.

Dynamic strain sweep tests were performed to search for the linear viscoelastic area of the paste, ranging

from 0.1% to 300% at a constant frequency of 6.28 rad·s^{-1}. Dynamic frequency sweep tests were processed in a frequency interval between 0.1 and 200 rad·s^{-1} within the linear viscoelastic region. The relevant rheological parameters could be obtained as a function of frequency that has intimate contact with the molecule structures of pastes.

Results and discussion

Printing qualities of the printing pastes

The results presented in Table 1 show that by using SA, CMS, and CMC as thickeners one can obtain excellent printing qualities, such as better screenability, higher color yield, and more even color and line. However, the sharp drawing lines are difficult to get using thickeners CMS and CMC. Therefore, CMS and CMC used as thickeners can only meet the requirement of large-area printing while not being fit for fine pattern printing in comparison with SA. In addition, thickener XG has the worst screenability, leading to white points, and a warp-lacking and weft-lacking pattern in the printing. Meantime, XG as a printing paste cannot achieve a bright and even color.

Paste rheology is a key factor for printing quality, which affects color, sharpness of mark, levelness, and color yield.[18] In order to tentatively explore the relations between rheology and the printability of paste, SA and XG are selected as two typical pastes that obtain the best and worst printing qualities, respectively. Their fluidity, thixotropy, and viscoelasticity will be extensively studied in the following sections.

Steady-shear characterization

As indicated in Figures 1 and 2, the flow curves of SA and XG solutions exhibit different shear-thinning behavior for the flow through the screen openings and penetration into the fibers. The Cross model[19] has been well used to describe the shear-thinning properties of SA solutions, in which the viscosity at infinite shear rate was neglected, since the high shear rate Newtonian viscosity was never approached in our study:

$$\eta = \frac{\eta_0}{\left[1+\left(\lambda\dot{\gamma}\right)^m\right]} \tag{7}$$

where $\dot{\gamma}$ is the shear rate (s^{-1}), η is the apparent viscosity (Pa·s), η_0 is the zero-shear viscosity (Pa·s), λ is time constant (s), and m is dimensionless constant, ruling the shear dependence in the shear-thinning region.

Meanwhile, it was found that the better fitting data were not obtained with the Cross model for XG solutions in our study. Nevertheless, the power-law model has been employed to depict the flow behavior of XG solutions with accuracy:

$$\eta = K\dot{\gamma}n^{-1} \tag{8}$$

where K represents the consistency coefficient (mPa·s^n) and n is flow index.

From the flow curves, SA solutions go through the transition from the Newtonian region to the power-law region, while XG solutions show a prominent shear-thinning feature and high viscosity at low shear rates

Table 1. The printing qualities of different printing pastes

Printing paste	Paste add-on (g m^{-2})	*K/S*	Color unevenness (%)	Thick line		Thin line	
				width (μm)	unevenness (%)	width (μm)	unevenness (%)
SA	81.6	7.571	4.24	1058	2.61	322	14.40
XG	52.7	3.971	10.68	796	24.10	222	28.38
CMS	92.6	10.142	4.90	1104	5.24	410	10.20
CMC	79.1	8.260	4.55	1146	2.89	413	11.92
FG	54.0	5.565	8.62	907	12.87	287	20.08
CG	55.9	0.783	3.33	929	10.69	271	22.07
GG	53.0	4.918	9.25	924	17.19	246	30.41
HGG	57.3	5.739	6.68	824	17.31	236	30.69
LBG	60.0	0.727	2.59	906	10.89	266	27.26

SA: sodium alginate; XG: xanthan; CMS: carboxymethyl starch; CMC: carboxymethylcellulose; FG: flaxseed gum; CG: carrageenan gum; GG: guar gum; HGG: hydroxypropyl guar gum; LBG: locust bean gum.

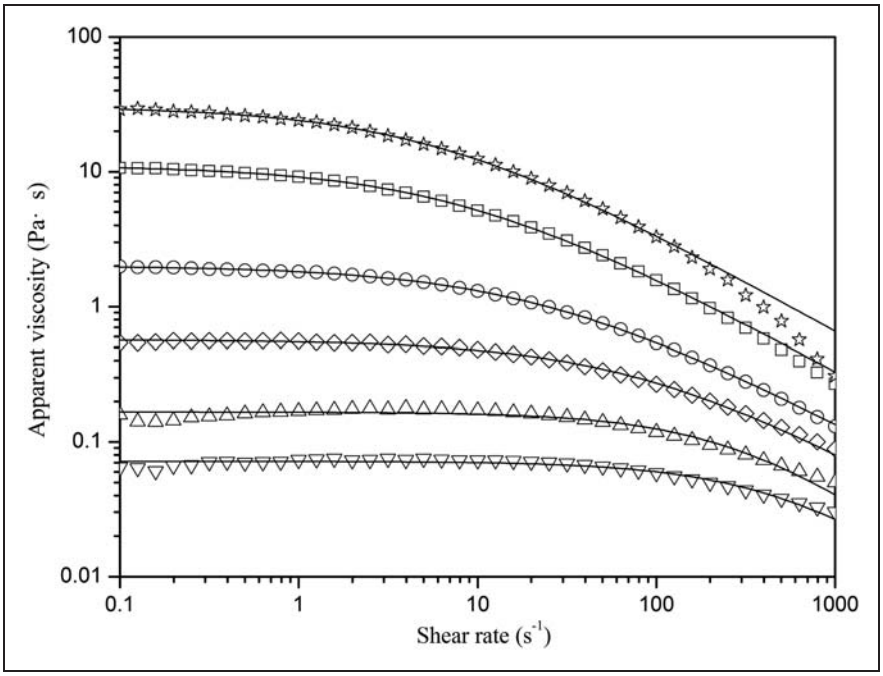

Figure 1. Apparent viscosity as a function of shear rate for sodium alginate in different concentrations at 25°C; symbols: (▽) 0.5%, (△) 0.7%, (□) 1%, (○) 1.4%, (◇) 2.1%, (☆) 3%; full lines represent the best fits of the Cross model.

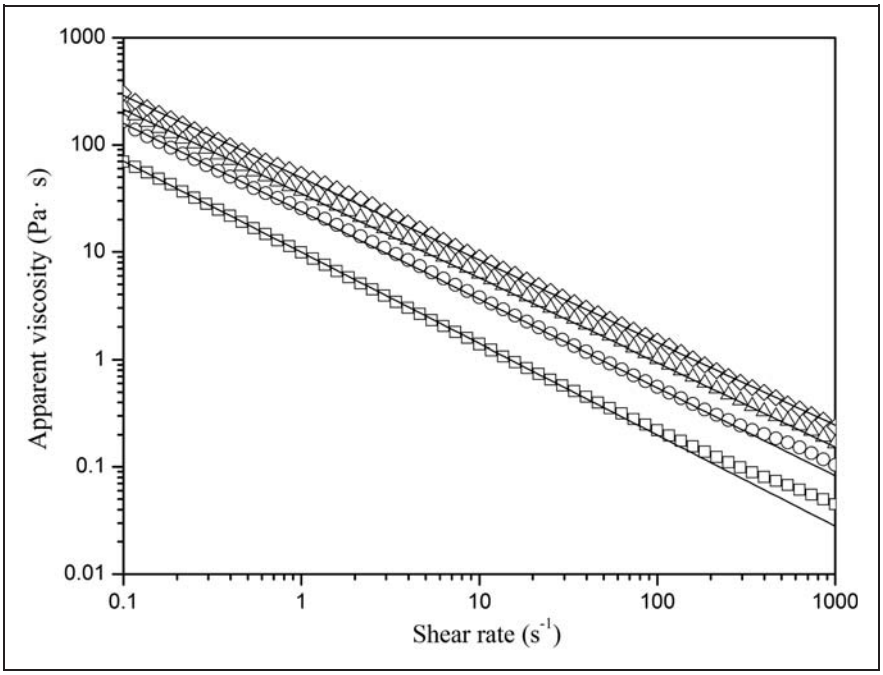

Figure 2. Apparent viscosity as a function of shear rate for xanthan in different concentrations at 25°C; symbols: (□) 0.7%, (○) 1.4%, (△) 2.1%, (◇) 3%; full lines represent the best fits of the power-law model.

and low concentrations. It may be attributed to the flexibility of the SA linear chain and the stiffness of the XG chain. The stiff molecules have a large hydrodynamic size, which contributes to high viscosity and pseudoplasticity.

Thixotropic properties

Thixotropy can be related to the build-up or breakdown of the structure of the paste system with time, having great impact upon the printing quality. The desirable properties for an easy application and a good performance of the paste are the immediate decrease of its viscosity under shear and the quick restoration of the original viscosity after the removal of shear.

From the thixotropic loop tests, the area enclosed by the hysteresis loop indicates the degree of structural breakdown due to shearing.[20] As shown in Figure 3, SA is characterized by a combined hysteresis loop, that is, an anticlockwise loop at low shear rates and a clockwise loop at higher shear rates ($\dot{\gamma} > 100\,s^{-1}$). The anticlockwise and clockwise loops are not clearly visible. By contrast, XG shows a relatively larger clockwise loop related to the larger structural viscosity that needs more time to restore the original level after shearing.

In addition, the in-shear structural recovery tests are also used to investigate the capability of the pastes to recover their original structure under low shear conditions after decomposition under high shear conditions.[16] The viscosity profiles as a function of time for SA and XG are given in Figure 4. Meanwhile, the quantitative results are shown in Table 2, from which it can be seen that XG returns to its original structure more slowly than SA does. That might be the reason why SA is suitable for printing fine motifs and outlines.

Dynamic viscoelastic characterization

Dynamic strain sweep tests. It has been seen from Figures 5 and 6 that SA and XG in the same concentration have very different viscoelastic properties with the increase of strain, which can be closely related to the particular molecular structures. With strain increasing, G'' of SA is larger than G'; after a plateau, the two moduli monotonously decrease, which is a classical behavior for a polymer solution. In addition, δ is constantly more than 60°, characterized by more viscous behavior and performing relatively stable viscoelasticity. This may be beneficial for SA to be pressed through the mesh and gain excellent color yield and levelness under the small changes of the printing process.

In comparison, XG shows a transformation from elasticity to viscosity. On the one hand, G' is about six times larger than G'' in the linear viscoelastic region, evidencing prominent elastic behavior against passing through the mesh. On the other hand, in the non-linear viscoelastic region G' decreases rapidly,

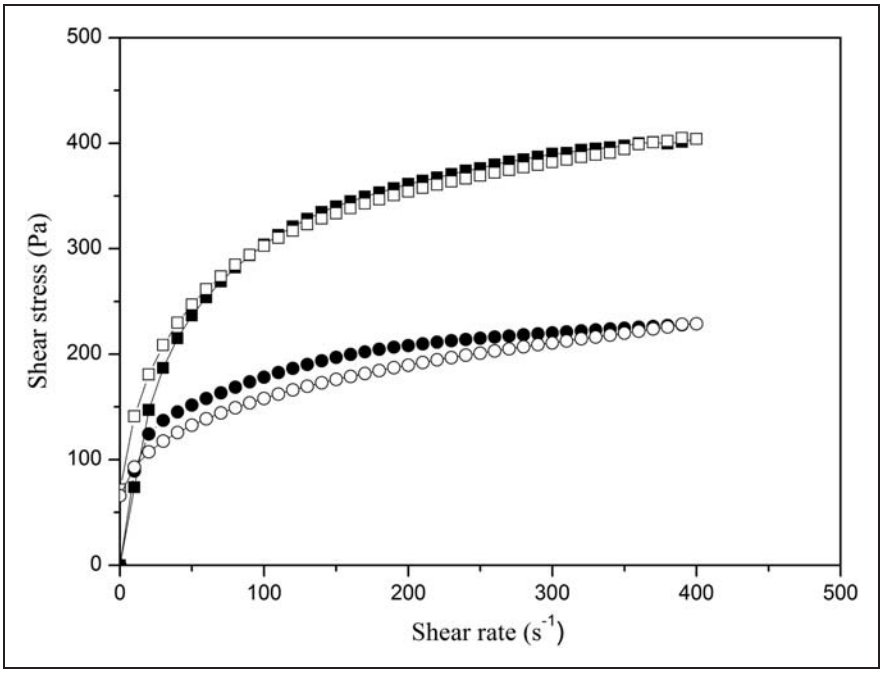

Figure 3. Thixotropic loop of the pastes at 25°C; symbols: 3 wt% sodium alginate (■) up, (□) down; 3 wt% xanthan (●) up, (○) down.

G'' increases to maximum, and δ goes through a remarkable increase from 8° to 70° with the increase of strain. When strain come up to certain values (>50%), XG exhibits more viscous behavior. Its viscoelasticity fluctuates to a large extent under external forces, which need more complex printing technology.

Dynamic frequency sweep tests. The dependence of G' and G'' on frequency can be used to characterize or classify dispersion.[21] The slope and the crossover of G' and G'' allow differentiation between a sol/solution, weak-gel structure or a dispersion particle system, such as suspensions, emulsions, and foams, and a crossover (G', G'') is an indicator of a weak-gel structure.[22]

Within the linear viscoelastic region, the effect of frequency on the viscoelasticity of the two thickeners will be discussed in the frequency ranging from 0.1 to 200 rad·s^{-1} at strain 3%. Two mechanical models were used to fit the experimental data: the Friedrich–Braun model and the Generalized Maxwell model. In the Friedrich–Braun model,[23] G' and G'' can be expressed as

$$G'(\omega) = G_e + \Delta G \frac{(\lambda_F\omega)^d\left[\cos\left(\frac{\pi}{2}d\right) + (\lambda_F\omega)^c\cos\left(\frac{\pi}{2}(d-c)\right)\right]}{1 + 2((\lambda_F\omega)^c\cos\left(\frac{\pi}{2}c\right) + (\lambda_F\omega)^{2c}} \tag{9}$$

$$G''(\omega) = \Delta G \frac{(\lambda_F\omega)^d\left[\sin\left(\frac{\pi}{2}d\right) + (\lambda_F\omega)^c\sin\left(\frac{\pi}{2}(d-c)\right)\right]}{1 + 2((\lambda_F\omega)^c\cos\left(\frac{\pi}{2}c\right) + (\lambda_F\omega)^{2c}} \tag{10}$$

where G_e is the equilibrium modulus when the frequency tends to zero, ΔG is a parameter that rules the magnitude of the viscoelastic response, λ_F is a characteristic time, and the exponents c and d are derivation orders of the differential operators.

Yet in the Generalized Maxwell model,[24] the values of the overall G' and G'', at any frequency, are given by the sum of four contributions from four Maxwell elements in parallel:

$$G'(\omega) = \frac{G_1(\omega\theta_1)^2}{1+(\omega\theta_1)^2} + \frac{G_2(\omega\theta_2)^2}{1+(\omega\theta_2)^2} + \frac{G_3(\omega\theta_3)^2}{1+(\omega\theta_3)^2} + \frac{G_4(\omega\theta_4)^2}{1+(\omega\theta_4)^2} \tag{11}$$

Table 2. In-shear recovery properties of 3 wt% sodium alginate (SA) and 3 wt% xanthan (XG) determined at 25°C

Pastes	Step 1 (Pa·s)	Step 2 (Pa·s)	Step 3 (Pa·s)	Recovery ratio (%)
SA	26.07 ± 0.06	1.01 ± 0.00	24.33 ± 0.09	93.33
XG	58.93 ± 0.12	0.60 ± 0.00	50.39 ± 0.05	85.51

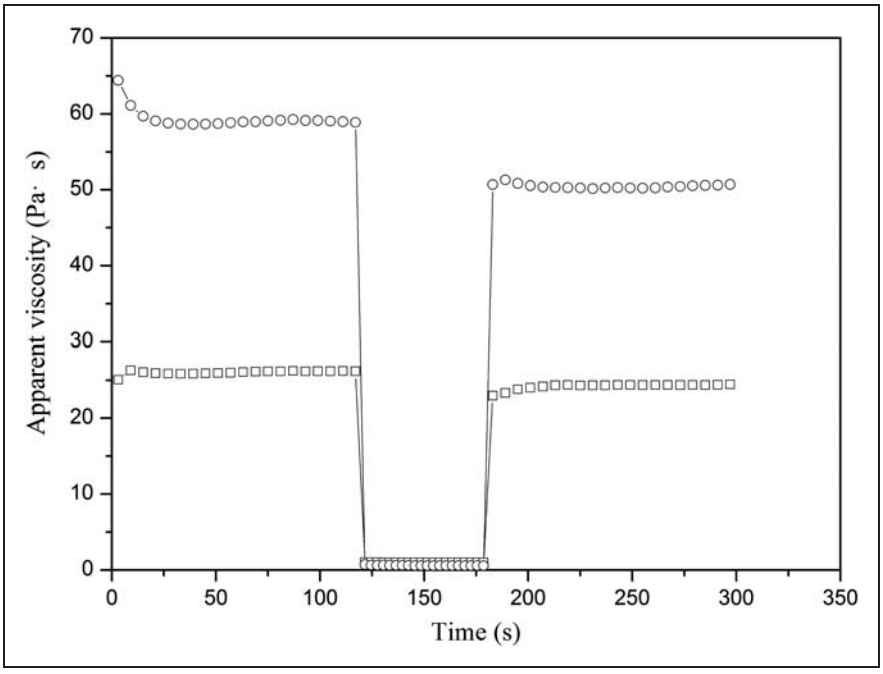

Figure 4. In-shear structural recovery of the pastes at 25°C; symbols: (□) 3 wt% sodium alginate, (○) 3 wt% xanthan.

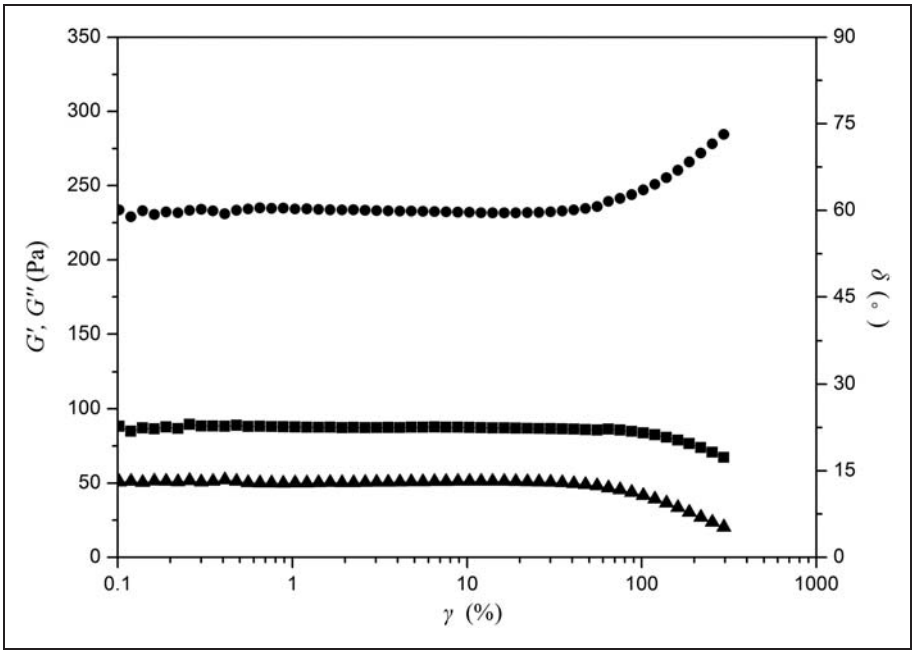

Figure 5. Storage modulus, G', loss modulus, G'', and loss angle, δ, as functions of strain, γ, for 3 wt% sodium alginate at 25°C; symbols: (▲) G', (■) G'', (●) δ.

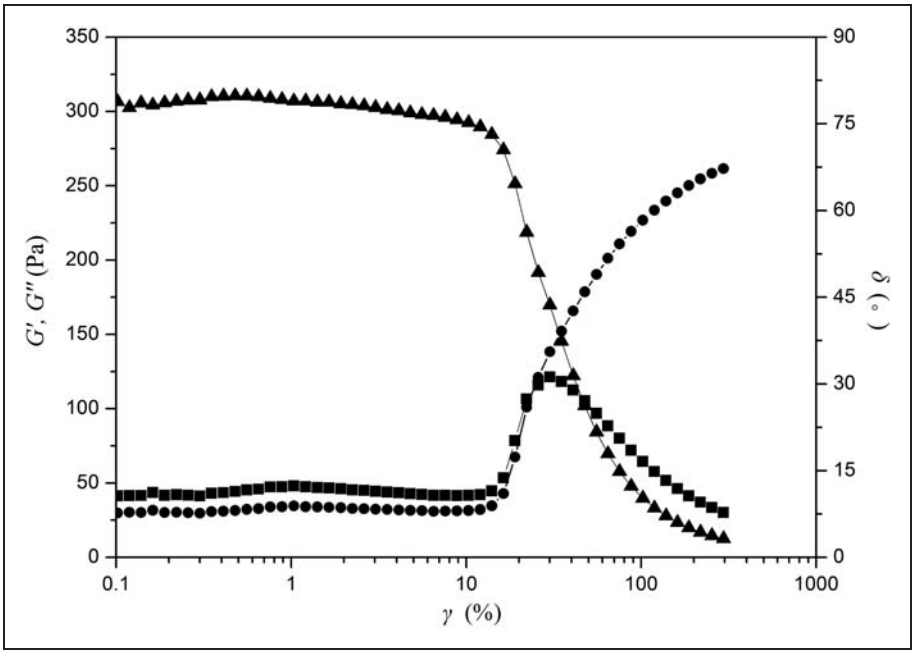

Figure 6. Storage modulus, G', loss modulus, G'', and loss angle, δ, as functions of strain, γ, for 3 wt% xanthan at 25°C; symbols: (▲) G', (■) G'', (●) δ.

$$G''(\omega) = \frac{G_1\omega\theta_1}{1+(\omega\theta_1)^2} + \frac{G_2\omega\theta_2}{1+(\omega\theta_2)^2} + \frac{G_3\omega\theta_3}{1+(\omega\theta_3)^2} + \frac{G_4\omega\theta_4}{1+(\omega\theta_4)^2} \quad (12)$$

where G_i is the elastic modulus, θ_i is the terminal relaxation time, and ω is the angular frequency.

The fitting results of two models to the experimental data are shown in Figure 7. The Friedrich–Braun model provides a better description of dynamic modulus

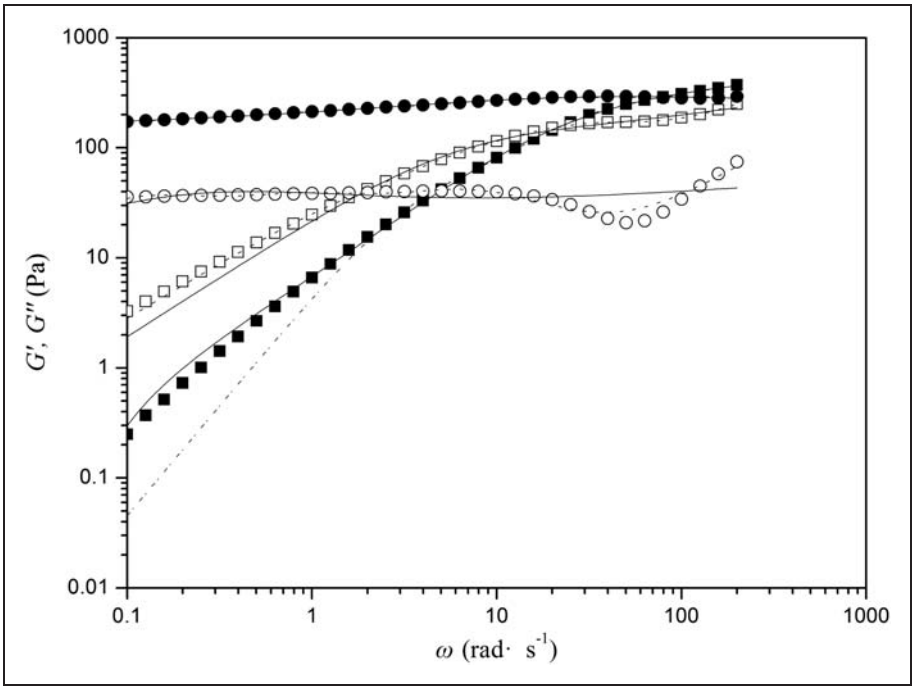

Figure 7. Storage modulus, G' and loss modulus, G'', as functions of angular frequency, ω, for the pastes at 25°C; symbols: 3 wt% sodium alginate (■) G', (□) G''; 3 wt% xanthan (●) G', (○) G''; full lines represent the best fits of the Friedrich–Braun model and dash lines those of the Generalized Maxwell model.

for SA, while the Generalized Maxwell model is better for XG.

The flow behavior of the paste through the screen openings is affected by elasticity. It was found that the most important factor determining the printability of screen printing pastes was frequency dependence of tan δ.[25] As can be seen from Figures 7 and 8, the viscoelastic behaviors of SA and XG have very significant differences in the same concentration. SA solution changes from viscosity to elasticity under the actions of frequency. The G'' is larger than G', and δ more than 45° within low frequency, indicating more viscous behavior. Later as frequency increases, G' increases more rapidly than G'' does until two curves reach an intersection ($G' = G''$). Whereafter, G' exceeds G'', and δ decreases to the minimum. By contrast, XG solution exhibits weak-gel behavior that G' is always superior to G'', and no crossover between these two moduli was observed throughout the measured frequency. This means that the elastic behavior dominates over the viscous component throughout the entire frequency range examined. These characterizations make it difficult to press through the screen openings and may lead to printing defects, such as poor screenability and a warp-lacking and weft-lacking pattern.

The viscoelastic behaviors of SA and XG are relevant to the different molecular structures. SA, a linear block copolymer, has a non-chemical crosslinking structure, forming a sol/solution system through physical entanglement. Nevertheless, XG solutions exist in the weak-gel structure due to the strong inter- and intra-molecular associations. The molecules composed of pentasaccharides repeating units may maintain an ordered, single-stranded helix conformation at room temperature in aqueous solution.[26]

Correlation between steady-shear and dynamic properties

According to the Cox–Merz rule, η^* measured with oscillatory rheometry is equal to η measured in steady-shear flow. Dynamic rheological properties can be compared with steady-shear rheological properties to provide insight structure of the paste:[27]

$$\eta(\dot{\gamma}) = |\eta^*(\omega)|_{\dot{\gamma}=\omega} \tag{13}$$

The flow and dynamic rheological data of SA and XG pastes are shown in Figure 9. The departure from the Cox–Merz rule presents in XG paste, which may be attributed to the hyperentanglement for structure decay due to the effect of the strain deformation applied to the system or to the existence of a weak-gel structure.[28]

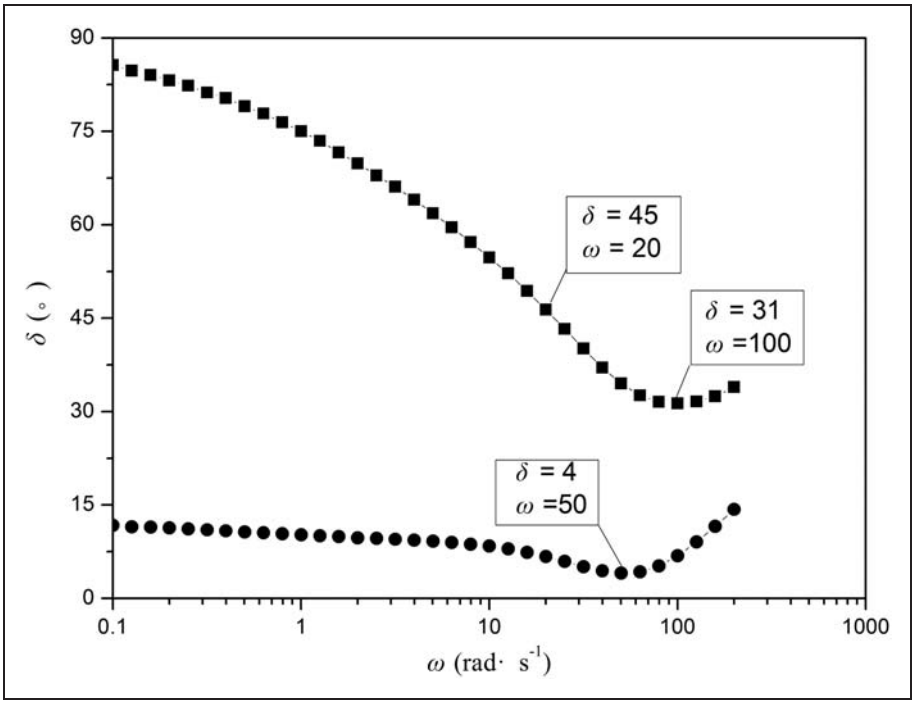

Figure 8. Loss angle, δ, as a function of angular frequency, ω, for the pastes at 25°C; symbols: (■) 3 wt% sodium alginate, (●) 3 wt% xanthan.

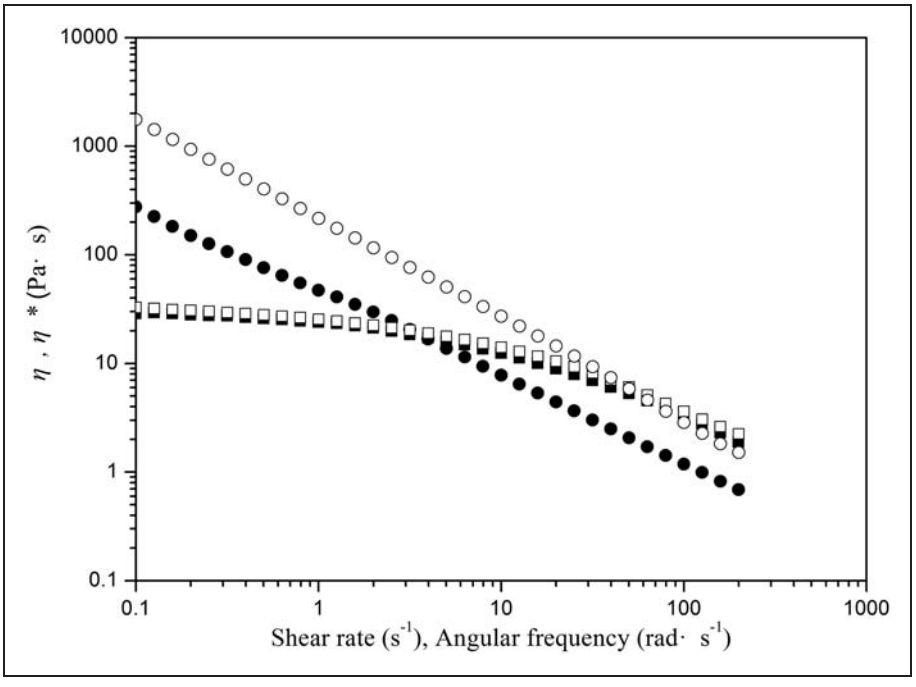

Figure 9. Cox–Merz plot for the pastes at 25°C; symbols: 3 wt% sodium alginate (■) η, (□) η^*; 3 wt% xanthan (●) η, (○) η^*.

Conclusions

Among nine polysaccharides, SA as a thickener can obtain the best printing qualities, while XG obtains the worst. Through the rheological measurements, it is found that SA and XG perform totally different rheological properties under external forces due to the unique chemical structures.

The steady-shear tests show that XG exhibits a more prominent shear-thinning feature in comparison with SA. The Cross model gives good description of apparent viscosity experimental data for SA, but the power-law model gives the best description for XG. In the transient tests, XG has more remarkable hysteresis thixotropy, and it is seen that the structural viscosity will need much more time to return to its original level after shears. From the dynamic tests, it can be drawn that SA is a thickener of more prominent viscous behaviors, beneficial for the quantity of printing paste applied to gain excellent color depth and levelness. By comparison, XG exhibits more elastic behaviors and a weak-gel characteristic, resulting in printing defects such as poor screenability and a warp-lacking and weft-lacking pattern. In addition, in the whole deformation process SA possesses relatively stable viscoelasticity, while XG experiences a transition from elasticity to viscosity. Furthermore, the viscoelastic data of SA and XG can be well correlated with the Friedrich–Braun model and the Generalized Maxwell model, respectively. The relationship between dynamic and steady-shear properties (the Cox–Merz rule) is satisfactory for SA while undesirable for XG.

It may be inferred that those who show weaker elasticity, stronger viscosity, relatively steady viscoelasticity, and the structural viscosity liable to restore the original level after shears may be more appropriate as the pastes to achieve better printing qualities on cotton printing with reactive dye.

Funding

This work was supported by the Key Laboratory of Science & Technology of Eco-Textile, Ministry of Education; College of Chemistry, Chemical Engineering & Biotechnology; Donghua University. It was also funded by the Innovation Foundation for PhD Candidate of Donghua University (CUSF-DH-D-2013046).

References

1. Lapasin R, Pricl S, Graziosi M, et al. Rheological properties of polysaccharide solutions and derived printing pastes in continuous and oscillatory flow conditions. *Ind Eng Chem Res* 1988; 27: 1802–1806.
2. Marco M, Moresi M and Sappino F. Rheological behavior of aqueous dispersions of algal sodium alginates. *J Food Eng* 1996; 28: 283–295.
3. Teli MD, Shanbag V, Dhande SS, et al. Rheological properties of amaranthus paniculates (rajgeera) starch vis-à-vis maize starch. *Carbohydr Polym* 2007; 69: 116–122.
4. Abo-Shosha MH, Ibrahim NA, Allam E, et al. Preparation and characterization of polyacrylic acid/karaya gum and polyacrylic acid/tamarind seed gum adducts and utilization in textile printing. *Carbohydr Polym* 2008; 74: 241–249.
5. Guion TH and Hood JR. Viscosity profiles of printing thickeners at high shear rates and their use in predicting paste flow in screen printing. *Textil Res J* 1985; 55: 498–508.
6. Šostar-Turk S and Schneider R. Printing properties of a high substituted guar gum and its mixture with alginate. *Dyes Pigm* 2000; 47: 269–275.
7. Fijan R, Basile M, Lapasin R, et al. Rheological properties of printing pastes and their influence on quality-determining parameters in screen printing of cotton with reactive dyes using recycled polysaccharide thickeners. *Carbohydr Polym* 2009; 78: 25–35.
8. Fijan R, Šostar-Turk S and Lapasin R. Rheological study of interactions between non-ionic surfactants and polysaccharide thickeners used in textile printing. *Carbohydr Polym* 2007; 68: 708–717.
9. Abdel-Halim ES, Emam HE and El-Rafie MH. Utilization of hydroxypropyl cellulose and poly (acrylic acid) – hydroxypropyl cellulose composite as thickeners for textile printing. *Carbohydr Polym* 2008; 74: 938–941.
10. Storz H and Müller KJ. Physicochemical features of ultra-high viscosity alginates. *Carbohydr Res* 2009; 344: 985–995.
11. Garciía-Ochoa F, Santos VE, Casas JA, et al. Xanthan gum: production, recovery, and properties. *Biotechnol Adv* 2000; 15: 549–579.
12. Hardalov I and Glucharov S. Rheological behaviour of alginate thickeners. *Melliand Textilber* 1988; 69: 906–909.
13. Choppe E, Puaud F, Nicolai T, et al. Rheology of xanthan solutions as a function of temperature, concentration and ionic strength. *Carbohydr Polym* 2010; 82: 1228–1235.
14. SmidsrØd O and Hang A. A light scattering study of alginate. *Acta Chem Scand* 1968; 22: 797–810.
15. Holzwarth G. Molecular weight of xanthan polysaccharide. *Carbohydr Res* 1978; 66: 173–186.
16. Mezger TG. Rotational tests. In: Zorll U (ed.) *The rheology handbook: For users of rotational and oscillatory rheometers*. Hannover: Vincentz, 2002.
17. Clasen C and Kulike WM. Determine of viscoelastic and rheo-optical material functions of water-soluble cellulose derivatives. *Prog Polym Sci* 2001; 26: 1839–1919.
18. Kumbasar EPA. Mixture printing pastes from high substituted guar gum and alginates on reactive printing of viscose. *J Appl Polym Sci* 2007; 103: 745–751.
19. Cross MM. Rheology of non-Newtonian fluids: a new flow equation for pseudoplastic systems. *J Colloid Sci* 1965; 20: 417–437.
20. Durairaj R, Ekere NN and Salam B. Thixotropy flow behaviour of solder and conductive adhesive pastes. *J Mater Sci Mater Electron* 2004; 15: 677–683.

21. Xu XJ, Xu J, Zhang YY, et al. Rheology of triple helical lentinan in solution: steady shear viscosity and dynamic oscillatory behavior. *Food Hydrocolloids* 2008; 22: 735–741.
22. Dongowski G, Drzikova B, Senge B, et al. Rheological behaviour of β-glucan preparations from oat products. *Food Chem* 2005; 93: 279–291.
23. Friedrich C and Braun H. Generalized Cole–Cole behavior and its rheological relevance. *Rheol Acta* 1992; 31: 309–322.
24. Doublier JL and Cuvelier G. Gums and hydrocolloids: functional aspects. In: Eliasson AC (ed.) *Carbohydrates in food*. New York: Marcel Dekker, Inc., 1996.
25. Hirai K, Ono K, Sakata T, et al. Structure and dynamic viscoelasticity of polyimide particles-dispersed pastes. *Nihon Reoroji Gakkaishi* 2000; 28: 85–89.
26. Tako M, Teruya T and Tamaki Y. Co-gelation mechanism of xanthan and galactomannan. *Colloid Polym Sci* 2010; 288: 1161–1166.
27. Da Silva JAL, Oliverita JC and Rao MA. Rheological properties of heated cross-linked waxy maize starch dispersions. *Int J Food Prop* 1998; 1: 23–34.
28. Alves VD, Freitas F, Costa N, et al. Effect of temperature on the dynamic and steady-shear rheology of a new microbial extracellular polysaccharide produced from glycerol byproduct. *Carbohydr Polym* 2010; 79: 981–988.